Sensors and Materials, Vol. 36, No. 2 (2024) 507–513
MYU Tokyo

S & M 3538

Scintillation Properties of Tb-doped $SrLu_2O_4$ Single Crystals

Hiromi Kimura,[1*] Hiroyuki Fukushima,[2] Kenichi Watanabe,[3] Takeshi Fujiwara,[1] Hidetoshi Kato,[1] Masahito Tanaka,[1] Takumi Kato,[4] Daisuke Nakauchi,[4] Noriaki Kawaguchi,[4] and Takayuki Yanagida[4]

[1]National Metrology Institute of Japan (NMIJ), National Institute of Advanced Industrial Science and Technology (AIST), 1-1-1 Umezono, Tsukuba, Ibaraki 305-8568, Japan
[2]Department of Electrical and Electronic Engineering, National Institute of Technology, Fukui College, Geshi-Cho, Sabae, Fukui 916-8507, Japan
[3]Department of Applied Quantum Physics and Nuclear Engineering, Kyushu University, 744 Motooka, Nishi, Fukuoka 819-0395, Japan
[4]Division of Materials Science, Nara Institute of Science and Technology (NAIST), 8916-5 Takayama, Ikoma, Nara 630-0192, Japan

(Received November 1, 2023; accepted January 17, 2024)

Keywords: radiation-induced luminescence, scintillators, photoluminescence, single crystals

Tb-doped $SrLu_2O_4$ single crystals were grown by the floating zone method, and their optical and scintillation properties were evaluated. Regarding the scintillation properties, all the prepared crystals showed the sharp emission peaks assigned to Tb^{3+} 4f–4f transitions in the range of 350–650 nm. The obtained decay times of 1.0–1.6 ms were typical values for the Tb^{3+} 4f–4f transitions. From the results of the pulse area spectra, the 1.0% Tb-doped crystal showed the highest light yield of 19600 photons/MeV among the prepared crystals.

1. Introduction

Scintillators are a type of luminescent material, and they immediately convert the absorbed energy of ionizing radiation into many low-energy photons. The combination of a scintillator and a photodetector is used for a typical scintillation detector,(1) which has been used in various applications including medical diagnosis,(2,3) security,(4) industrial inspection,(5) and environmental monitoring.(6–8) The performance of scintillation detectors depends primarily on the scintillation properties, and the required scintillation properties vary depending on the applications. Therefore, many types of scintillator have been reported in the form of single crystals,(9–16) ceramics,(17–21) and glasses.(22–31)

Until the 1990s, UV-blue emitting scintillators have been mainly studied because a photomultiplier tube (PMT), which has a high sensitivity in the UV-blue region, has mainly been used as a photodetector in scintillation detectors.(32–34) In the 2000s, with the progress of Si-based photodetectors, two-dimensional X-ray detectors including flat panel detectors (FPDs)(35–37) and X-ray line scan cameras(38,39) have attracted considerable attention. They consist of scintillators and Si-based photodetectors, and the required properties of scintillators

*Corresponding author: e-mail: h.kimura@aist.go.jp
https://doi.org/10.18494/SAM4767

ISSN 0914-4935

for the above detectors were high effective atomic number (Z_{eff}), high light yield (*LY*), high density, low fading, and green-to-red emission.[40] Tl-doped CsI crystals (Z_{eff}: ~54, *LY*: ~54000 photons/MeV),[41] $CdWO_4$ crystals (Z_{eff}: ~66, *LY*: ~20000 photons/MeV),[42,43] and Ce, Pr-doped GOS ceramics (Z_{eff}: ~60, *LY*: ~30000 photons/MeV)[44] were utilized as scintillators in the FPD and X-ray line scan cameras. However, there are no green-to-red emitting scintillators with large Z_{eff} and high light yield, and thus the development of new scintillators is expected.

Tb-doped $SrRE_2O_4$ (RE = rare-earth ions) has a high potential for scintillators because when RE = Lu, Z_{eff} and density are ~65 and 8.4 g/cm^3, respectively.[45–49] In our previous research, Tb-doped SrY_2O_4 single crystals showed green emission bands, and the estimated light yields were 12000 photons/MeV.[50] However, there are no reports on the scintillation properties of Tb-doped $SrLu_2O_4$. In this study, we investigated the optical and scintillation properties of Tb-doped $SrLu_2O_4$ single crystals.

2. Experimental Methods

$SrLu_2O_4$ single crystals doped with various concentrations of Tb were grown by the floating zone technique.[46,51] The raw powders of Tb_4O_7 (99.99%, Furuuchi Chemical), $SrCO_3$ (99.99%, Wako Pure Chemical), and Lu_2O_3 (99.999%, Nippon Yttrium) were mixed in a stoichiometric ratio. Here, the concentrations of Tb were 0.1, 0.5, 1.0, and 2.0 mol% with respect to Lu. The mixture was annealed at 1200 °C for 8 h to desorb carbon dioxide, and then the mixture was formed to a cylindrical shape by cold isostatic pressing at 15 MPa for 15 min. The cylindrical ceramic was sintered at 1400 °C for 8 h using an electric furnace, and the crystal growth was performed using a floating zone (FZ) furnace (Crystal Systems, FZ-T-12000-X-VPO-PC-YH). As growth conditions, the pulling speed and rotation rate were 10 mm/h and 20 rpm, respectively. The surfaces of the obtained crystals were mechanically polished to evaluate the optical and scintillation properties.

To identify the structure phase, X-ray diffraction (XRD) patterns were measured using a diffractometer (Rigaku, MiniFlex400). As optical properties, diffuse transmittance spectra, photoluminescence (PL) excitation/emission maps, and PL decay curves were evaluated using a spectrometer (Shimadzu, SolidSpec-3700), a Quantaurus-QY (Hamamatsu Photonics, C11347), and a Quantaurus-τ (Hamamatsu Photonics, C11367), respectively.

For the measurement of the scintillation spectra and decay curves, we used our previously reported original systems.[52,53] To calculate the scintillation light yields, the pulse area spectra of a ^{137}Cs γ-ray source using the prepared crystals were observed using our customized setup,[54] which can be measured using the scintillators with lifetimes in the ms range.

3. Results and Discussion

Figure 1 shows the XRD patterns of Tb-doped $SrLu_2O_4$ single crystals and the standard card of $SrLu_2O_4$ (JCPDS: 00-032-1242). All the diffraction patterns matched the reference data for an orthorhombic structure of $SrLu_2O_4$. Since other diffraction peaks were not confirmed, we have successfully prepared the single phase of $SrLu_2O_4$ by the FZ method. Figure 2 shows the

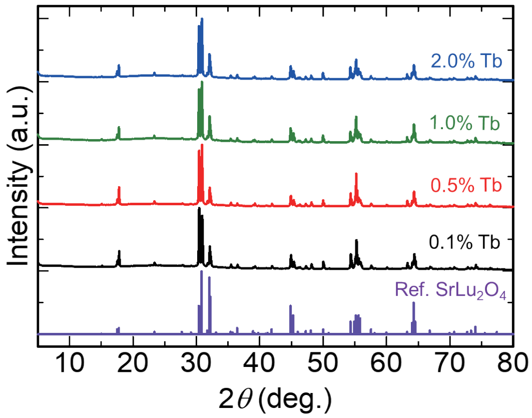

Fig. 1. (Color online) XRD patterns of Tb-doped $SrLu_2O_4$ single crystals and standard cards of $SrLu_2O_4$ (JCPDS: 00-032-1242).

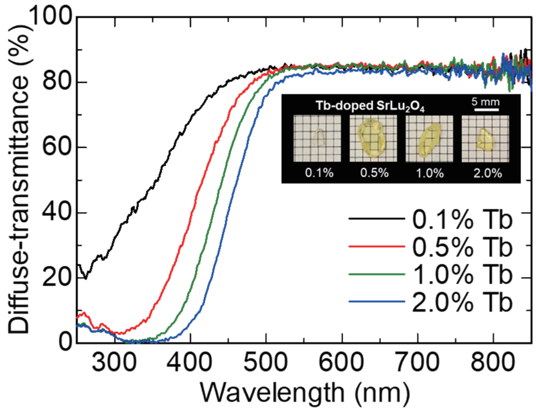

Fig. 2. (Color online) Diffuse-transmittance spectra of Tb-doped $SrLu_2O_4$ single crystals. (Inset) Photographs of Tb-doped $SrLu_2O_4$ single crystals.

diffuse-transmittance spectra of Tb-doped $SrLu_2O_4$ single crystals. All the crystals have a high transmittance of ~80% in the wavelength range from 450 to 850 nm. The decrease in transmittance was confirmed at wavelengths below 450 nm, and absorption bands were shifted to longer wavelengths with increasing Tb concentration. In previous reports on Tb-doped phosphors, absorption bands appeared at around 290 and 550 nm, which were associated with the Tb^{3+} 4f–5d and charge transfer (CT) transitions between O^{2-} and Tb^{4+}, respectively.(47,48,55–58)

PL excitation/emission maps and quantum yield (*QY*) values of the Tb-doped $SrLu_2O_4$ single crystals are shown in Fig. 3. All the Tb-doped crystals exhibited several sharp emission peaks in the wavelength range of 350–650 nm under excitation at 290 nm. The excitation spectral peak around 290 nm corresponds to the absorption band of the Tb^{3+} 4f–5d transition (as shown in Fig. 2). Since the same spectral positions of emission peaks were confirmed in previous reports on Tb-doped phosphors, the emission peaks were attributed to Tb^{3+} 4f–4f transitions.(49,59,60) With increasing Tb concentration, the emission intensity decreased below 500 nm, which would be due to the effect of the self-absorptions of Tb^{4+} and Tb^{3+}. The *QY* of the 0.1% Tb-doped crystal (29.4%) was the highest among the prepared Tb-doped crystals, and this value was higher than that of Pr-doped $SrLu_2O_4$ crystals (~18.4%), which were the same host material.(46)

Under an excitation of 265 nm, the PL decay curves of Tb-doped $SrLu_2O_4$ single crystals monitored at 550 nm are shown in Fig. 4. A single exponential decay function was used to approximate the decay curves except for the instrumental response functions (IRFs) and the rise part of each decay curve. The derived lifetimes were 1.8–2.3 ms for Tb-doped $SrLu_2O_4$ crystals, which were reasonable for Tb^{3+} 4f–4f transitions.(7,49,59–61) In $SrLu_2O_4$ with low Tb concentration, the increase in rise time was observed. This trend was also confirmed in previous reports on Tb-doped SrY_2O_4 single crystals, which was attributed to the cross-relaxation process between neighboring Tb^{3+} ions.(50,62–64)

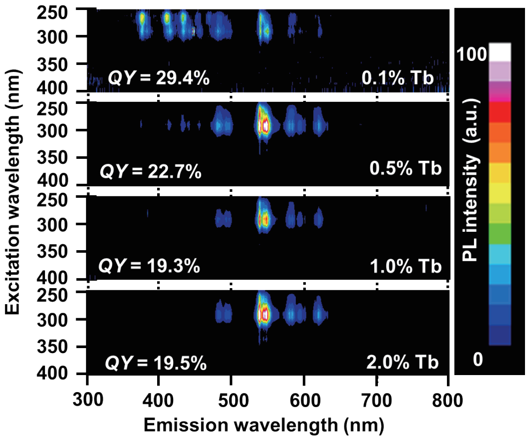

Fig. 3. (Color online) PL excitation/emission maps and *QY* values of Tb-doped $SrLu_2O_4$ single crystals.

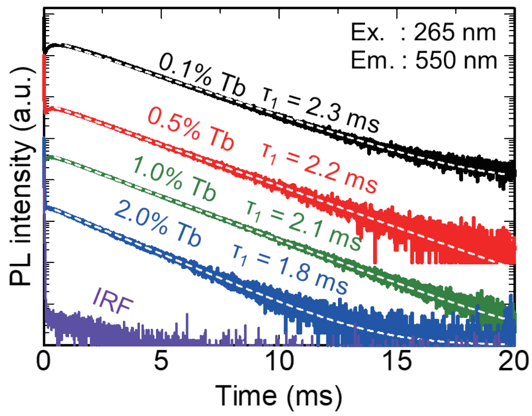

Fig. 4. (Color online) PL decay curves of Tb-doped $SrLu_2O_4$ single crystals monitored at 550 nm under an excitation of 265 nm.

Figure 5 shows the X-ray-induced scintillation properties of Tb-doped $SrLu_2O_4$ single crystals. All the crystals showed several sharp peaks originating from Tb^{3+} 4f–4f transitions, and the spectral features were similar to the results in PL. In a previous report, the nondoped $SrLu_2O_4$ crystal showed a broad emission peak around 300–500 nm due to self-trapped excitons,(46) whereas this was not observed in Tb-doped crystals. The 0.1% Tb-doped crystal showed several sharp emission peaks in the wide range of 350–650 nm. In the 0.5–2.0% Tb-doped $SrLu_2O_4$ single crystals, the green emission was mainly observed because of the effect of the self-absorptions of Tb^{4+} and Tb^{3+}, which was suitable for the wavelength sensitivity of Si-based photodetectors. Figure 6 shows the X-ray-induced scintillation decay curves of Tb-doped $SrLu_2O_4$ single crystals. The decay curves can be fitted with a single exponential decay function except for the IRF. The decay time constants were 1.0–1.6 ms, which were typical values for Tb^{3+} 4f–4f transitions under X-ray irradiation.(65,66)

The pulse area spectra of Tb-doped $SrLu_2O_4$ single crystals and the BGO scintillator under γ-ray irradiation from a ^{137}Cs source are shown in Fig. 7. The commercial BGO scintillator, which has a *LY* of ~8200 photons/MeV,(67) was used as the reference. For the 0.1, 0.5, 1.0, and 2.0% Tb-doped crystals, a full-energy absorption peak appeared at the channels of 745, 277, 175, and 108, respectively. Considering a full-absorption peak position of the BGO (263 ch), the calculated *LY*s of the 0.1, 0.5, 1.0, and 2.0% Tb-doped crystals were 16100, 19600, 12400, and 7600 photons/MeV, respectively. Here, the quantum efficiencies (QEs) of the PMT to emission peak wavelengths at 415 nm ($QE = 36\%$ for 0.1% Tb-doped crystals), 480 nm ($QE = 25\%$ for BGO), and 545 nm ($QE = 11\%$ for 0.5, 1.0, and 2.0% Tb-doped crystals) were taken into consideration. The *LY* of the 1.0% Tb-doped $SrLu_2O_4$ single crystal was higher than that of Tb-doped SrY_2O_4 single crystals (~12000 photons/MeV) in our previous report.(50) In contrast, the *LY* of Tb-doped $SrLu_2O_4$ crystals was lower than that of the commercial Tl-doped CsI scintillators (*LY*: ~54000 photons/MeV) for the FPD.(41)

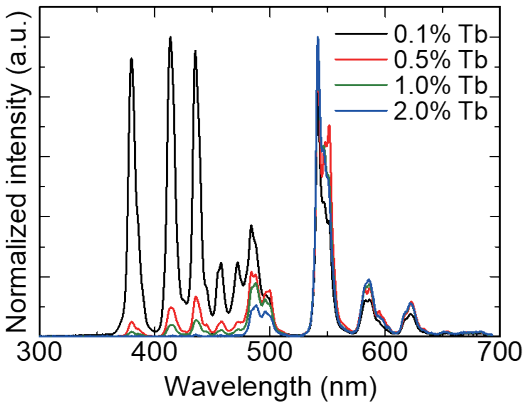

Fig. 5. (Color online) X-ray-induced scintillation properties of Tb-doped $SrLu_2O_4$ single crystals.

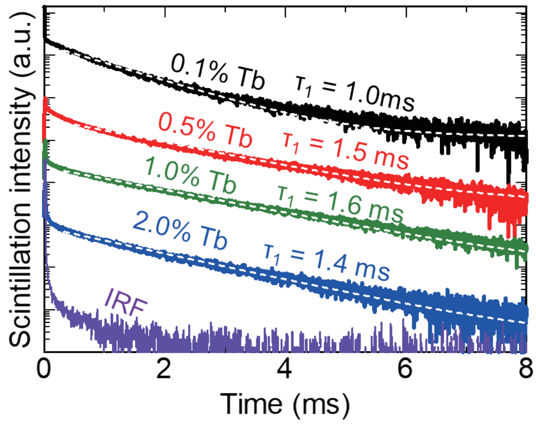

Fig. 6. (Color online) X-ray-induced scintillation decay curves of Tb-doped $SrLu_2O_4$ single crystals.

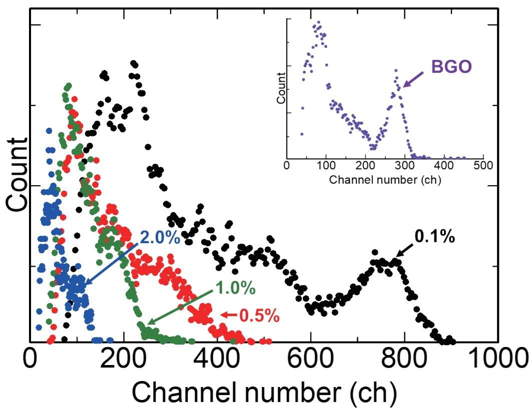

Fig. 7. (Color online) Pulse area spectra of Tb-doped $SrLu_2O_4$ single crystals under γ-ray irradiation from a ^{137}Cs source. The inset shows the pulse area spectrum of a commercial $Bi_4Ge_3O_{12}$ (BGO) scintillator as the reference.

4. Conclusions

The structure and optical and scintillation properties of Tb-doped $SrLu_2O_4$ single crystals were investigated. From XRD results, all the prepared crystals had the single phase of $SrLu_2O_4$. Under 290 nm excitation and X-ray irradiation, several emission lines appeared in the range of 350–650 nm, and emission origins were Tb^{3+} 4f–4f transitions. With increasing Tb concentration, spectral shapes were changed by the self-absorptions of Tb^{4+} and Tb^{3+}. Since the 0.5, 1.0, and 2.0% Tb-doped $SrLu_2O_4$ single crystals exhibited strong green emission peaks around 540 nm, they were suitable for the wavelength sensitivity of the Si-photodiode. Among the prepared crystals, the light yield of the 1.0% Tb-doped $SrLu_2O_4$ crystal was the highest (~19600 photons/MeV), which is higher than that of a commercial BGO scintillator (~8000 photons/MeV).

Acknowledgments

This work was supported by Grants-in-Aid for Scientific Research A (22H00309), Scientific Research B (21H03733 and 22H02939), and Research Activity Start-up (22K20489). The Cooperative Research Project of the Research Center for Biomedical Engineering is also acknowledged.

References

1 T. Yanagida: Proc. Japan Acad. Ser. B **94** (2018) 75.
2 S. Yamamoto, S. Okumura, N. Kato, and J. Y. Yeom: J. Instrum. **10** (2015) T09002.
3 K. Shinsho, R. Oh, M. Tanaka, N. Sugioka, H. Tanaka, G. Wakabayashi, T. Takata, W. Chang, S. Matsumoto, G. Okada, S. Sugawara, E. Sasaki, K. Watanabe, Y. Koba, K. Nagasaka, S. Yoshihashi, A. Uritani, and T. Negishi: Jpn. J. Appl. Phys. **62** (2023) 010502.
4 J. Glodo, Y. Wang, R. Shawgo, C. Brecher, R. H. Hawrami, J. Tower, and K. S. Shah: Phys. Procedia **90** (2017) 285.
5 C. Connolly: Sens. Rev. **28** (2008) 194.
6 K. Watanabe, T. Yanagida, K. Fukuda, A. Koike, T. Aoki, and A. Uritani: Sens. Mater. **27** (2015) 269.
7 P. Kantuptim, T. Kato, D. Nakauchi, N. Kawaguchi, K. Watanabe, and T. Yanagida: Sens. Mater. **35** (2023) 451.
8 K. Watanabe: Jpn. J. Appl. Phys. **62** (2023) 010507.
9 T. Suto, N. Kawano, K. Okazaki, Y. Takebuchi, H. Fukushima, T. Kato, D. Nakauchi, and T. Yanagida: Jpn. J. Appl. Phys. **62** (2023) 010610.
10 H. Fukushima, D. Nakauchi, T. Kato, N. Kawaguchi, and T. Yanagida: Sens. Mater. **35** (2023) 429.
11 M. Arai, Y. Fujimoto, M. Koshimizu, H. Kimura, T. Yanagida, and K. Asai: Mater. Res. Bull. **120** (2019) 110589.
12 D. Shiratori, H. Fukushima, D. Nakauchi, T. Kato, N. Kawaguchi, and T. Yanagida: Sens. Mater. **35** (2023) 439.
13 C. Dujardin, E. Auffray, E. Bourret-Courchesne, P. Dorenbos, P. Lecoq, M. Nikl, A. N. Vasil'ev, A. Yoshikawa, and R.-Y. Zhu: IEEE Trans. Nucl. Sci. **65** (2018) 1977.
14 M. J. Weber: J. Lumin. **100** (2002) 35.
15 T. Yanagida, T. Kato, D. Nakauchi, and N. Kawaguchi: Jpn. J. Appl. Phys. **61** (2022) SB1040.
16 N. Kawaguchi, T. Kato, D. Nakauchi, and T. Yanagida: Jpn. J. Appl. Phys. **62** (2023) 010611.
17 T. Kunikata, T. Kato, D. Shiratori, P. Kantuptim, D. Nakauchi, N. Kawaguchi, and T. Yanagida: Sens. Mater. **35** (2023) 491.
18 N. Kawaguchi, H. Kimura, D. Nakauchi, T. Kato, and T. Yanagida: Jpn. J. Appl. Phys. **61** (2022) SB1004.
19 N. J. Cherepy, Z. M. Seeley, S. A. Payne, E. L. Swanberg, P. R. Beck, D. J. Schneberk, G. Stone, R. Perry, B. Wihl, S. E. Fisher, S. L. Hunter, P. A. Thelin, R. R. Thompson, N. M. Harvey, T. Stefanik, and J. Kindem: Proceedings Volume 9593, Hard X-Ray, Gamma-Ray, and Neutron Detector Physics XVII, L. Franks, R. B. James, M. Fiederle, and A. Burger, Eds. (2015) 95930P.
20 D. Nakauchi, F. Nakamura, T. Kato, N. Kawaguchi, and T. Yanagida: Sens. Mater. **35** (2023) 467.
21 H. Kimura, T. Kato, T. Fujiwara, M. Tanaka, D. Nakauchi, N. Kawaguchi, and T. Yanagida: Jpn. J. Appl. Phys. **62** (2023) 010504.
22 D. Shiratori, H. Fukushima, D. Nakauchi, T. Kato, N. Kawaguchi, and T. Yanagida: Jpn. J. Appl. Phys. **62** (2023) 010608.
23 H. Kimura, T. Fujiwara, M. Tanaka, T. Kato, D. Nakauchi, N. Kawaguchi, and T. Yanagida: Sens. Mater. **35** (2023) 513.
24 V. Dormenev, A. Amelina, E. Auffray, K.-T. Brinkmann, G. Dosovitskiy, F. Cova, A. Fedorov, S. Gundacker, D. Kazlou, M. Korjik, N. Kratochwil, V. Ladygin, V. Mechinsky, M. Moritz, S. Nargelas, R. W. Novotny, P. Orsich, M. Salomoni, Y. Talochka, G. Tamulaitis, A. Vaitkevicius, A. Vedda, and H.-G. Zaunick: Nucl. Instrum. Methods Phys. Res. Sect. A **1015** (2021) 165762.
25 Y. Takebuchi, D. Shiratori, T. Kato, D. Nakauchi, N. Kawaguchi, and T. Yanagida: Sens. Mater. **35** (2023) 507.
26 L. Q. Nguyen, G. Gabella, B. L. Goldblum, T. A. Laplace, J. S. Carlson, E. Brubaker, and P. L. Feng: Nucl. Instrum. Methods Phys. Res. Sect. A **988** (2021) 164898.
27 H. Kimura, T. Kato, D. Nakauchi, N. Kawaguchi, and T. Yanagida: Sens. Mater. **34** (2022) 691.
28 N. P. Giha, W. M. Steinberger, L. Q. Nguyen, J. S. Carlson, P. L. Feng, S. D. Clarke, and S. A. Pozzi: Nucl. Instrum. Methods Phys. Res. Sect. A **1014** (2021) 165676.

29 H. Masai, Y. Yanagida, H. Kawamoto, Y. Koguchi, M. Koshimizu, and M. Yamawaki: Sens. Mater. **34** (2022) 699.
30 G. Ito, H. Kimura, D. Shiratori, D. Nakauchi, T. Kato, N. Kawaguchi, and T. Yanagida: Sens. Mater. **34** (2022) 685.
31 K. Shinozaki, G. Okada, N. Kawaguchi, and T. Yanagida: Jpn. J. Appl. Phys. **62** (2023) 010603.
32 D. R. Schaart: Phys. Med. Biol. **66** (2021) 09TR01.
33 M. R. Farukhi: IEEE Trans. Nucl. Sci. **29** (1982) 1237.
34 E. Roncali, M. A. Mosleh-Shirazi, and A. Badano: Phys. Med. Biol. **62** (2017) R207.
35 S. Izumi, S. Kamata, K. Satoh, and H. Miyai: IEEE Trans. Nucl. Sci. **40** (1993) 158.
36 I. G. Valais, I. S. Kandarakis, D. N. Nikolopoulos, I. A. Sianoudis, N. Dimitropoulos, D. A. Cavouras, C. D. Nomicos, and G. S. Panayiotakis: IEEE Trans. Nucl. Sci. **52** (2005) 1830.
37 T. Fujiwara, H. Miyoshi, Y. Mitsuya, N. L. Yamada, Y. Wakabayashi, Y. Otake, M. Hino, K. Kino, M. Tanaka, N. Oshima, and H. Takahashi: Rev. Sci. Instrum. **93** (2022) 013304.
38 K. Hyun Kim, H. Yeon Yeo, and I. Sub Jun: J. Nucl. Sci. Technol. **45** (2008) 435.
39 L. Nagornaya, V. Ryzhikov, A. Apanasenko, I. Tupitsyna, V. Chernikov, and V. Vostretsov: Nucl. Instrum. Methods Phys. Res. Sect. A **486** (2002) 268.
40 E. Kotter and M. Langer: Eur. Radiol. **12** (2002) 2562.
41 M. Jeong and M. Hammig: Nucl. Eng. Technol. **52** (2020) 2572.
42 M. Moszynski, M. Balcerzyk, M. Kapusta, A. Syntfeld, D. Wolski, G. Pausch, J. Stein, and P. Schotanus: IEEE Trans. Nucl. Sci. **52** (2005) 3124.
43 H. Nanto: Sens. Mater. **30** (2018) 327.
44 T. Yanagida: Opt. Mater. **35** (2013) 1987.
45 L. M. Lopato: Ceramurg. Int. **2** (1976) 18.
46 H. Fukushima, D. Nakauchi, T. Kato, M. Koshimizu, N. Kawaguchi, and T. Yanagida: Solid State Sci. **110** (2020) 106471.
47 E. Pavitra, G. S. R. Raju, Y. H. Ko, and J. S. Yu: Phys. Chem. Chem. Phys. **14** (2012) 11296.
48 R. K. Tamrakar and K. Upadhyay: J. Electron. Mater. **47** (2018) 651.
49 J. Zhang, Y. Wang, L. Guo, and Y. Huang: J. Am. Ceram. Soc. **95** (2012) 243.
50 H. Kimura, H. Fukushima, K. Watanabe, T. Fujiwara, M. Tanaka, D. Nakauchi, T. Kato, N. Kawaguchi, and T. Yanagida: Jpn. J. Appl. Phys. **63** (2024) 01SP21.
51 H. Fukushima, D. Nakauchi, T. Kato, N. Kawaguchi, and T. Yanagida: Opt. Mater. **128** (2022) 112385.
52 T. Yanagida, K. Kamada, Y. Fujimoto, H. Yagi, and T. Yanagitani: Opt. Mater. **35** (2013) 2480.
53 T. Yanagida, Y. Fujimoto, T. Ito, K. Uchiyama, and K. Mori: Appl. Phys. Express **7** (2014) 062401.
54 K. Watanabe, T. Yanagida, D. Nakauchi, and N. Kawaguchi: Jpn. J. Appl. Phys. **60** (2021) 106002.
55 Z. Aoki, Y. Takebuchi, D. Nakauchi, T. Kato, N. Kawaguchi, and T. Yanagida: J. Mater. Sci. Mater. Electron. **34** (2023) 2021.
56 J. Zmojda, M. Kochanowicz, P. Miluski, and D. Dorosz: Fibers **2** (2014) 150.
57 A. K. V. Raj, P. Prabhakar Rao, S. Divya, and T. R. Ajuthara: Powder Technol. **311** (2017) 52.
58 R. Oka, T. Nouchi, and T. Masui: Colorants **1** (2022) 347.
59 Z. Aoki, Y. Takebuchi, D. Nakauchi, T. Kato, N. Kawaguchi, and T. Yanagida: Opt. Mater. **134** (2022) 113068.
60 K. Ichiba, Y. Takebuchi, H. Kimura, T. Kato, D. Nakauchi, N. Kawaguchi, and T. Yanagida: Sens. Mater. **35** (2023) 475.
61 D. Nakauchi, H. Fukushima, T. Kato, N. Kawaguchi, and T. Yanagida: Sens. Mater. **34** (2022) 611.
62 T. O. Sales, R. J. Amjad, C. Jacinto, and M. R. Dousti: J. Lumin. **205** (2019) 282.
63 Y. Liu, J. Zhang, C. Zhang, J. Jiang, and H. Jiang: J. Phys. Chem. C **120** (2016) 2362.
64 S. Kalusniak, E. Castellano-Hernández, H. Yalçinoğlu, H. Tanaka, and C. Kränkel: Appl. Phys. B **128** (2022) 33.
65 N. Kawano, T. Kato, G. Okada, N. Kawaguchi, and T. Yanagida: Opt. Mater. **73** (2017) 364.
66 N. Kawano, M. Akatsuka, H. Kimura, G. Okada, N. Kawaguchi, and T. Yanagida: Radiat. Meas. **117** (2018) 52.
67 I. Holl, E. Lorenz, and G. Mageras: IEEE Trans. Nucl. Sci. **35** (1988) 105.